

COMPARISON OF NINE IMAGE CLASSIFICATION METHODS ON LANDSAT 7 IMAGERY

Victor STRÎMBU*

Norwegian University of Live Sciences, Department of Ecology and Natural Resource Management,
Høgskoleveien 12, 1430 Ås, Norway, e-mail: victor.strimbu@nmbu.no

Vlad STRÎMBU

University of Alberta, Faculty of Agricultural, Life and Environmental Sciences, Department of Renewable Resources,
University of Alberta 2-14 Agriculture Forestry Centre, Edmonton, AB Canada T6G 2P5, e-mail: trimbu@ualberta.ca

Wesley PALMER

Louisiana Tech University, Colege of Applied and Natural Sciences, School of Forestry,
Louisiana Tech University, P. O. Box 10138, Ruston, LA 71272, USA, e-mail: wpalmer@latech.edu

Jean GOURD

Louisiana Tech University, Colege of Engineering and Science, Department of Computer Science
Louisiana Tech University, Nethken Hall 247, Ruston, LA 71272, USA, e-mail: jgourd@latech.edu

Abstract: Nine different widely used classification methods available in ArcGIS and ERDAS software packages were tested on Landsat 7 imagery with the objective to compare their performance and adequacy in classifying six major land cover elements: urban/commercial, residential, bare soil, vegetation, forest and water. A brief background for each classification method was provided, after which the results of each algorithm were visually compared and analyzed. Finally, the kappa coefficient was used as a quantitative metric to assess the agreement between methods. This study showed that different results are obtained when using different classification methods; in consequence the classification method must be carefully selected according to the objective and the available data. The finality of this work is to provide the average GIS software user with the understanding on how the classification method impacts the classification result, and a starting point in deciding what GIS software tool would be more appropriate given a certain context and goal.

Key words: ArcGIS, ERDAS Imagine, gis, landsat, land cover, remote sensing

* * * * *

INTRODUCTION

Remotely sensed image classification is central to obtaining reliable land use and land cover information, with applications in urban planning (Lu & Weng, 2006; Pinho et al., 2012), agriculture (Vibhute & Bodhe, 2012), forest management (Fu et al., 2010) and ecological

* Corresponding Author

management (Vannier et al., 2011). Moreover, the growing threat of climate change demands accurate periodical land cover information, which has become crucial for understanding the environment dynamics (Pielke, 2005).

Regardless of the application field, image classification has been performed ever since the onset of the information age, as a semi-automated or automated process, allowing the possibility to process large amounts of data fast and at a limited cost. On the down side, as with any other machine vision process, the accuracy is a matter of concern that must be evaluated and maximized. When performing multispectral image classification, there are several impediments that may hamper the quality of the results. Some originate in the quality of the remotely sensed image, some have to do with parameterization and the way a user operates a classification tool and some are inherent in the particular classification algorithm. Here we focus on the latter case simply because it cannot be circumvented. The primary objective of this paper is to compare nine different classification methods featured by two widely used GIS software packages: ArcGIS and ERDAS.

In the first section of the paper we provide some background information on the concept and mathematical construction of each method. In the second section, each classifier is used on an complex Landsat 7 satellite image, with the objective of identifying six landcover classes. Lastly we compare the results using visual and quantitative methods and try to provide the GIS user the information necessary to select the appropriate tool.

BACKGROUND

Image Classification

Image classification is the process that categorizes the image pixels into meaningful classes with the purpose to identify regions with similar qualities. In remote sensing, image classification is applied to satellite or aerial imagery with the aim to create a thematic map. As remotely sensed imagery usually features multiple spectral bands, the classification is performed in a multidimensional space with as many dimensions as there are bands. In terms of general classification strategies, it can be divided into two: supervised classification and unsupervised classification. The supervised strategy is aided by the user through establishing the target classes and providing their spectral signatures. The unsupervised classification on the other hand, attempts to group the pixels without any prior knowledge of the target classes. In the case of the unsupervised classification the procedure is equivalent to clustering and the two terms may be used interchangeably.

Supervised Classification

Supervised classification relies on the availability of a predefined number of classes as well as training data for each class. In the case of multi-band image classification, the training data consists of certain image regions that are known to belong to a particular class. A so called class signature is derived from each training region. The classification procedure uses these known class signature to decide the class membership of each image pixel.

Maximum Likelihood

Maximum Likelihood (ML) classification uses the mean and standard deviation of the training samples for each class (figure 1). For this reason it relies on the assumption that the training data are normally distributed. Every pixel is classified based on the maximum probability calculated from the normal distributions of each class. When the class proportions are known, it is possible to define a priori probabilities in order to facilitate decisions for those pixels with relatively close probabilities of belonging to more classes. In addition, the ArcGIS implementation allows the user to specify the percentage of pixels to be left out when the probability of belonging to any of the classes is small. It is the only supervised classifier offered by ArcGIS.

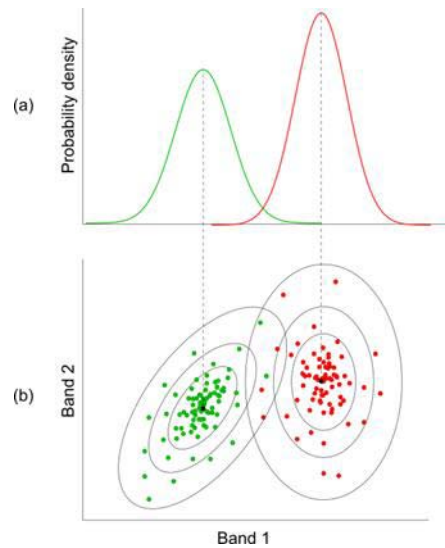


Figure 1. Probability distribution functions (a) of normally distributed training samples (b) for two different classes depicted here in green and red. Here only two bands are illustrated for better visualization

Mahalanobis Distance

The Mahalanobis Distance (MhD) classifier works on the assumption that the pixel values of each band are normally distributed. The Mahalanobis distance between every pixel and a class is calculated by: $MhD = (X - M_c)^T [(Cov)_c]^{-1} (X - M_c)$, where c identifies a particular class, X is the measurement vector of the candidate pixel, M_c is the mean vector of the signature of class c , $[(Cov)]_c$ is the covariance matrix of the pixels in the signature of class c , and T is the transposition function. Each pixel will be assigned to the class that minimizes MhD.

Minimum Distance

The Minimum Distance (MD) classifier assigns pixels to classes based only on Euclidian distance between the pixel coordinate in the multiband hyperspace and the mean signature of the class. It is the simplest rule for unsupervised classification and does not make any assumptions on how data or class signatures are distributed. Every pixel will be assigned to the class that minimizes the distance: $MD = \sqrt{\sum_{i=1}^n ((\mu_{ci} - X_i))^2}$, where n is the number of bands (dimensions), i identifies a particular band, c identifies a class, X_i is the value of the candidate pixel in band i , and μ_{ci} is the mean signature value of the class c in band i .

Spectral Angle Mapper

Spectral angle mapper (SAM) is based on the fact that pixels of the same class may have significant spectral distance between them due to different degrees of illumination. This classifier is invariant to illumination intensity and may be used on composite images of heterogeneous illumination and contrast. In SAM classification every pixel is assigned to the class with which it forms a minimal spectral angle (figure 2). The spectral angle is similar for those pixels that maintain a constant proportion between values in different bands. In other words the intensity recorded by each band is not important as long as inter-band value ratio is maintained.

Spectral Correlation Mapper

The Spatial Correlation Mapper (SCM) is an improvement of SAM published by de Carvalho and Meneses in 2000 (Carvalho & Meneses, 2000). It differs from SAM in the fact that it normalizes and centers the data in the mean of each spectrum. Furthermore, it uses the cosine of the spectral angle, making it very similar to the Pearsonian Correlation Coefficient.

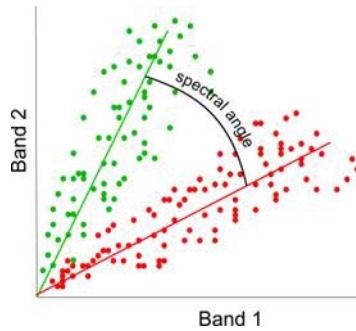


Figure 2. The spectral angle formed between training samples of two different classes: green and red. For illustrative purpose only two bands are used

Unsupervised Classification

The unsupervised strategy is entirely automated and for this reason the number of resulting classes is unknown. In general, the number of classes may be controlled to a certain degree through parameterization, but in most cases manual post processing is necessary to obtain the desired classification. As a rule of thumb, the number of classes resulted after unsupervised classification must be greater than the target number of classes. This way the target classes may be obtained by merging several unsupervised classes. Unsupervised classification is also used when the desired classes are not prior known and the user is responsible for the semantics of the resulting classes. Unsupervised classification has its theoretical foundation and is closely related to and cluster analysis, and for this reason some of the methods bear the term clustering.

K-means Clustering

K-means clustering algorithm is one of the most used clustering procedures having the merit to be simple and effective. It was first described by James MacQueen in 1967 (MacQueen, 1967). Performing k-means clustering requires the number of clusters to be known a priori. K-means clustering minimizes: $\sum_{j=1}^k \sum_{i=1}^n \|x_i^{(j)} - c_j\|^2$, where c_j is centre of cluster j and $x_i^{(j)}$ is the i -th data point (or pixel) that belongs to cluster j .

Algorithm 1. Pseudocode for k-means clustering. Parameters: K - number of clusters, I_MAX - maximum number of iterations, and ACS_Th - average cluster centre shift threshold (convergence threshold)

$I := 0$

place K cluster centres randomly

REPEAT

assign data points to the cluster with nearest centre

recalculate cluster centroid based on its constituent data points

ACS = average cluster centre shift from the previous iteration

$I := I + 1$

UNTIL ($I = I_MAX$) OR ($ACS < ACS_Th$)

ISODATA

ISODATA (Iterative Self Organising Data) is an iterative algorithm that performs unsupervised classification by a series of merging and splitting operations on data clusters. Unlike k-means, the number of resulting clusters or classes is not known a priori.

Algorithm 2. Pseudocode for ISODATA clustering. Parameters: N0 – initial number of clusters, SD_Th - threshold on the standard deviation within a cluster, CD_Th - threshold on the cluster centre distance, M_MAX - maximum number of merges per iteration, I_MAX - maximum number of iterations, ACD_Th - threshold on the average cluster centre distance, ACCD_Th - threshold on the average change in cluster centre distance (convergence threshold)

I := 0

place N0 random cluster centres and assigning each pixel to the nearest cluster

REPEAT

split clusters with standard deviation greater than SD_Th

merge a maximum of M_MAX clusters with centre distance smaller than CD_Th

recompute centre and standard deviations for the newly formed clusters

ACD = the average cluster centre distance

ACCD = the average change in cluster centre distance from previous iteration

I = I+1

UNTIL (I=I_MAX) OR (ACD<ACD_Th) OR (ACCD<ACCD_Th)

ArcGIS IsoCluster

Although it claims to be an implementation of ISODATA, the ArcGIS tool implements k-means clustering followed by some post processing filtering. ArcGIS uses the term „*migrating means technique*” to describe this unsupervised clustering method. At the end of the iterative process, when the clusters have reached a stable state, their number is reduced by eliminating those consisting in few pixels and by merging those with similar statistical properties.

The IsoCluster tool allows three parameters: the initial number of classes, the minimum pixels in a class and the sampling interval.

LANDSAT Imagery

The LANDSAT program is the longest running program for acquiring satellite imagery of the Earth. The first satellite was launched in 1972 and has since launched 7 more with the latest in 2013, providing a data continuity of over 40 years. The present study is using imagery acquired by the LANDSAT 7 satellite. The spatial platform is equipped with sensors that swipe the Earth surface with a swath of 183 km and acquire data on eight different spectrum bands (Table 1)

In terms of temporal resolution, the capture periodicity for a single scene varies with geographic location and priority, but for the USA territory, it is 16 days.

Table 1. The eight bands of LANDSAT 7. NIR = near infrared, SWIR = short wave infrared, TIR = thermal infrared, PAN = panchromatic

Band #	Designation	Wavelength (µm)	Resolution (m)
1	Blue	0.45-0.52	30
2	Green	0.52-0.60	30
3	Red	0.63-0.69	30
4	NIR	0.77-0.90	30
5	SWIR	1.55-1.75	30
6	TIR	10.40-12.50	60 (30)
7	SWIR	2.09-2.35	30
8	PAN	0.52-0.90	15

Kappa Statistic

Cohen's kappa coefficient (more widely known as kappa statistic) represents a common measure for assessing the inter-rater agreement for categorical data. It was first introduced by Cohen (1960) and it is used in many scientifically fields, including land cover image classification (Stehman, 1997).

Kappa statistic intends to give a quantitative measure of the magnitude of agreement between two or more raters. It is based on how much agreement is occurring (observed agreement) compared to how much agreement would be expected due to chance alone (expected agreement). It is calculated as: $k = \frac{P(O) - P(E)}{1 - P(E)}$, where $P(O)$ is the proportion of times the raters agree (observed agreement) and $P(E)$ is the proportion of times the raters are expected to agree by chance alone. Considering the above formula, kappa can range from 0 to 1, with 0 corresponding to agreement due only to chance and 1 to complete agreement. Viera and Garrett (2005) provide a good overview of kappa statistic.

METHODS

Data

The multispectral data used in this study was collected by LANDSAT 7 on October 6, 1999 above an area around Houston, Texas. This area was chosen because it features a balanced land variation, with a significant proportion of urban and residential areas, as well as forests, agriculture and a large body of water. The exact location of the study area is given in table 2. The Enhanced Thematic Mapper (ETM) package consists of nine images (including two different 30m resolution interpolations for the TIR band) out of which only eight were used for this study. The PAN image was excluded to maintain a consistent resolution and to ease pixel matching.

Table 2. Geographic coordinates of the four image corners

Corner	Latitude	Longitude
Upper-left	31.26051	-96.09261
Upper-right	31.29639	-93.58842
Lower-left	29.32488	-96.03241
Lower-right	29.35811	-93.57694

Classification

By visually inspecting the image we decided to perform the classifications in six classes: urban, residential, soil, vegetation, forest and water. An objective assessment requires that both ArcGIS and ERDAR tools use the same training set for the supervised classification. For this purpose, more than 50 polygons enclosing regions of known nature have been created in ArcGIS. The shapefile was saved and converted to areas of interest (AOI) for the ERDAS IMAGINE software. The strategy for unsupervised classification is to create a large number of subclasses that may be merged subsequently to form the six established classes.

ArcGIS Methodology

ArcGIS provides two tools for the supervised and unsupervised classification respectively: Maximum Likelihood and IsoCluster. We used the default parameters for both and set the initial number of clusters to 30 for IsoCluster.

IsoCluster produced 18 classes. Each has been inspected by overlapping the RGB composite image as well as relevant separate bands to decide what classes should be merged to finally obtain the six established classes. Nine of the initial classes were eliminated either because they represented deficient band overlap on the edge of the image or because they had few pixel members. The remaining number of classes was distributed so that urban, residential and vegetation had a one-to-one correspondence, forest and water were each formed by merging three classes, and soil had no correspondence.

ERDAS IMAGINE Methodology

ERDAS IMAGINE features two unsupervised classification methods: k-means clustering and ISODATA, and six supervised classification methods: Maximum likelihood, Mahalanobis Distance, Minimum Distance, Spectral Angle Mapper and Spectral Correlation Mapper.

While the default parameterization was used for supervised classification, the following parameters and processing was needed for the unsupervised classification. For k-means 30 cluster centers were set and for ISODATA the interval from 10 to 40. In addition, ISODATA used the following parameters (see background section for parameter meaning):SD_Th = 5, CD_Th = 4, M_MAX = 10, I_MAX =100 and ACCD_Th = 0.95.

Out of 30 classes produced by k-means: two were disqualified, three were merged into urban, one formed the residential, one formed the soil, five were merged into vegetation, 17 were merged to form the forest, and finally one corresponded to water.

ISODATA produced 40 subclasses that were grouped as follows: 26 disqualified, two urban, one residential, four soil, two vegetation, three forest, two water.

Assessment

Due to the lack of reliable synchronic reference land cover map for the particular area, the classified images were initially visually inspected, with a focus on certain critical regions. We discussed the observations and attempted to explain particularities of each classification by the underlying algorithm and band characteristics of the LANDSAT 7 images. To formally assess the difference between every pair of classified images, kappa statistic was used for a total of 36 pairs. Each algorithm was considered a rater and each pair had a corresponding kappa statistic. The information processing and kappa coefficient was calculated using package raster (Hijmans, 2014) and package irr (Gamer et al., 2012) on R statistical platform (R Core Team, 2013).

RESULTS AND DISCUSSION

General Classification Quality

ArcGIS IsoCluster

IsoCluster classification (figure 3) performed well in reciprocal separation of residential and urban areas, in the sense that few urban areas were classified as residential and vice versa. On the downside, one of the initially produced classes contained pixels in both residential areas and the majority of Lake Anahuac. Indeed Lake Anahuac has a distinct spectral signature in the visible spectrum (i.e. grey) due to its impurity. Even though the NIR band clearly distinguishes this body of water, IsoCluster was not able to classify it together with other bodies of water. The reason behind this is the relative intensity of the bands. The RGB bands are all well contrasted and they will have a more decisive influence on the unsupervised classification. The biggest shortcoming with this method is its inability to identify any of the soil pixels. Bare soil parcels and recently deforested land were incorrectly classified as urban. Forest and vegetation regions are often interspersed. This may be due to post classification filtering where smaller classes have been merged with vegetation class instead of forest. Conversely, some of the vegetation and planted agricultural land was classified as residential.

ArcGIS Maximum Likelihood

Compared to IsoCluster, the ArcGIS implementation of Maximum Likelihood (figure 4) did better in classifying the urban area with the exception of including waterland and some soil parcels that were especially bright in the visible spectrum. Interestingly, for some soil parcels, only the more humid regions were confused with urban area. The vegetation and forest areas were in general compact with only few interspersed regions. It did classify most of the bare soil parcels with the exception of those with high reflectance in the visible spectrum and the more humid ones. While large bodies of water were well delineated, rivers and small lakes were poorly classified. Vegetation was highly interspersed with soil pixels. The residential areas took over some of the less vigorous forested land. This is explained by the training samples, with residential areas being often rich in roadside trees. For this reason, the signature for the residential area featured high variability and was not normally distributed. Since it featured both buildings and trees, it was probably a bimodal distribution, in violation of Maximum Likelihood's primary assumption.

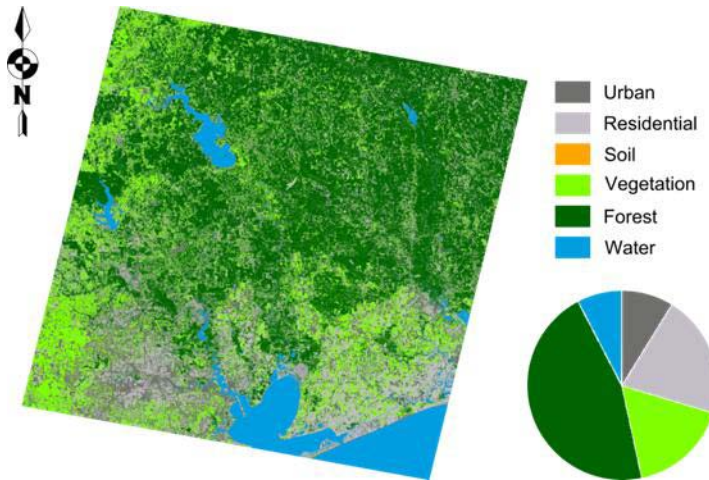


Figure 3. Land cover map produced by ArcGIS IsoCluster classifier

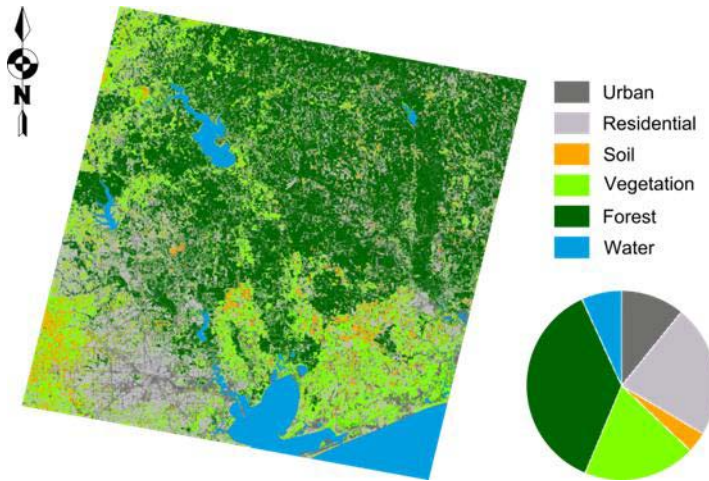


Figure 4. Land cover map produced by ArcGIS maximum likelihood classifier

ERDAS IMAGINE k-means

K-means clustering (figure 5) did an overall good segmentation. The algorithm performed especially well in classifying the water, even thin river lines, small lakes and pools. In regards to urban/residential delineation, the urban area is a bit too extensive, taking over regions that should be classified as residential. A few soil parcels as well as sandy river banks and ocean shore were also classified as urban. The downtown area where tall buildings shadow adjacent areas was erroneously classified as water contoured with forest pixels. Since both shadow and water has a low intensity response on all reflected spectra it was included in the same cluster. It may be extrapolated as a general disadvantage for unsupervised classification where the user cannot explicitly indicate a region's class.

ERDAS IMAGINE ISODATA

ISODATA clustering (figure 6) seemed to be the most appropriate algorithm for this particular data set, yielding the best classification overall. The few errors that it introduced were by classifying a few grasslands and cultivated land as residential, and the downtown as water. In

addition, a high number of soil patches were present in the urban and residential areas. It is unlikely that they all represent construction and development sites.

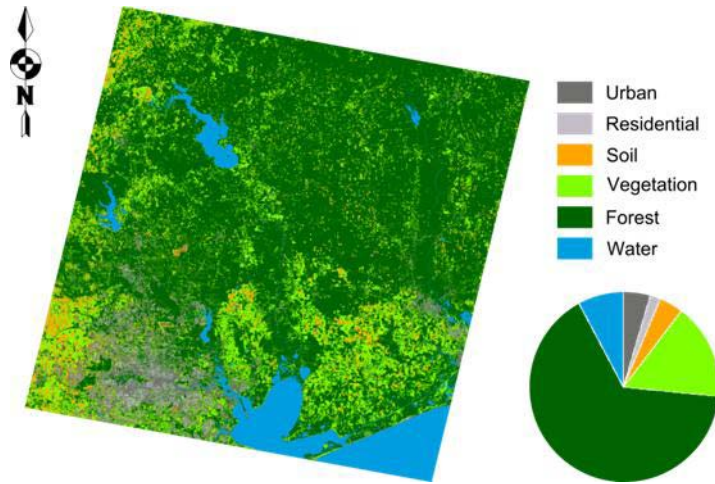


Figure 5. Land cover map produced by ERDAS IMAGINE k-means classifier

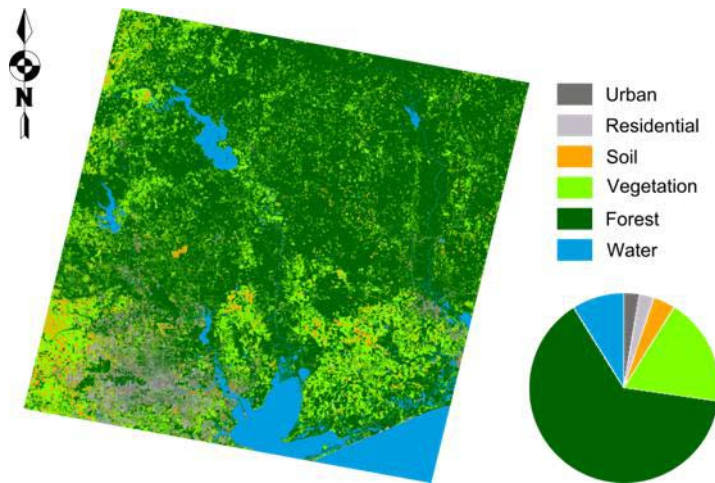


Figure 6. Land cover map produced by ERDAS IMAGINE ISODATA classifier

ERDAS IMAGINE Maximum Likelihood

As expected (figure 7), it performed nearly the same with the similar tool in ArcGIS. Despite the deterministic nature of maximum likelihood classification, some differences at the pixel level were observed.

ERDAS IMAGINE Mahalanobis Distance

Here (figure 8), the downtown area was correctly classified as urban but this may be due to the fact that small water bodies are classified as urban as well. Water in general is poorly delineated and often heavily intruded by the urban class. It is safe to say that Mahalanobis Distance shares most of the Maximum Likelihood shortcomings with the tendency to exaggerate them. Forest has little commission but has some significant omission, in general being intruded by the residential class. Soil is well classified.

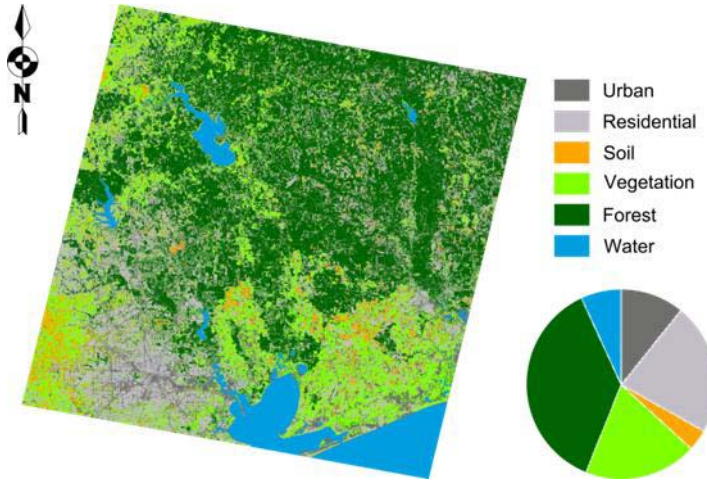


Figure 7. Land cover map produced by ERDAS IMAGINE maximum likelihood classifier

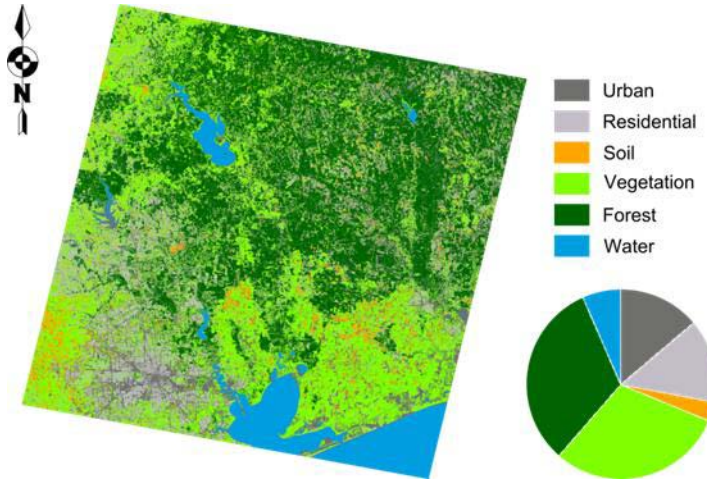


Figure 8. Land cover map produced by ERDAS IMAGINE Mahalanobis distance classifier

ERDAS IMAGINE Minimum Distance

With MD classifier (figure 9) water is very well contoured and forest is decently classified. On the downside, a large proportion of soil parcels were reclassified as urban and a large portion of vegetation were reclassified as residential. There were soil pixels on urban areas and vice versa. It seemed that Minimum Distance performs especially well in differentiating those pixels with high contrast in a single band even when the rest of the bands hold values that are close to a certain class signature. Inherently, Euclidian distance will have higher magnitude when measured along a single axis. Water for instance, has a stark contrast in the NIR band, making it easy to extract its afferent pixels.

ERDAS IMAGINE Spectral Angle Mapper

With SAM classifier (figure 10), forest is particularly well classified, and water too. Similar to the MD classifier, SAM classifies a large portion of soil and waterland as residential. The soil regions are further affected by scattered vegetation pixels. High intensity soil regions are classified as urban. Similarly, shore sand is wrongfully classified as urban where a soil classification would have been more appropriate. Nevertheless both soil and vegetation classifications are improved compared to MD.

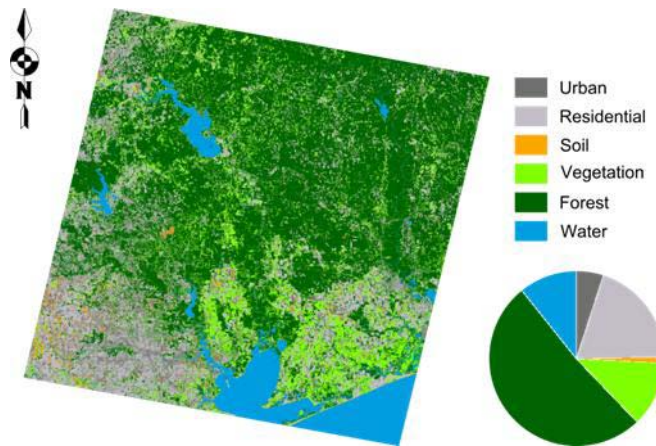


Figure 9. Land cover map produced by ERDAS IMAGINE minimum distance classifier

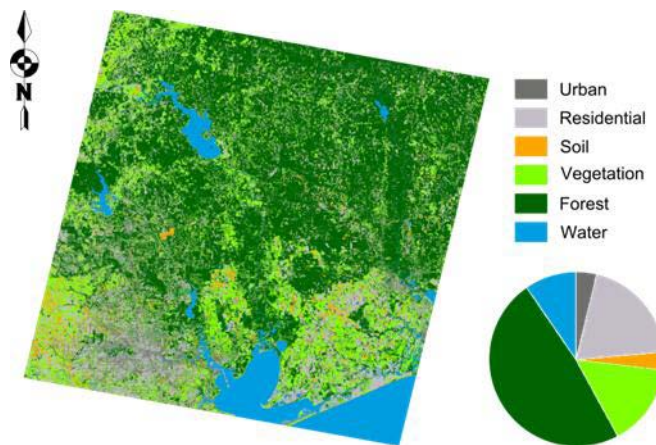


Figure 10. Land cover map produced by ERDAS IMAGINE Spectral Angle Mapper classifier

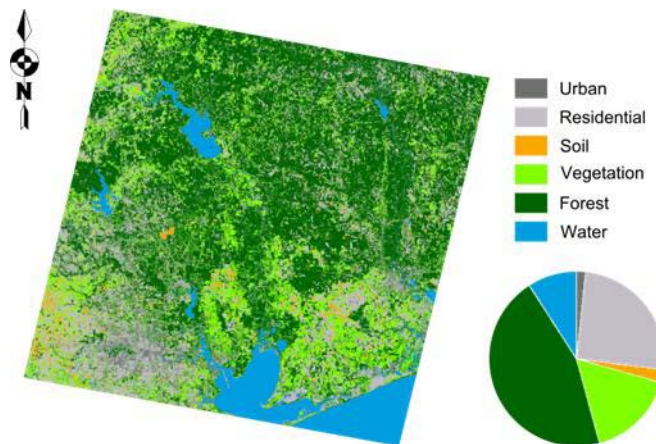


Figure 11. Land cover map produced by ERDAS IMAGINE Spectral Correlation Mapper classifier

ERDAS IMAGINE Spectral Correlation Mapper

Although Spectral Correlation Mapper has been proposed as an improvement to SAM, it performed slightly worse on this particular dataset (figure 11). There were an increased proportion of forest pixels in residential areas. In the same time the forest is significantly scattered with vegetation pixels. The residential area intruded more of the deforested land. The soil regions were less classified as urban but instead much more residential areas intruded. The water was slightly better delineated with the cost of more buildings shaded areas being classified as water. An improvement from SAM could be observed in the urban classification which is more compact.

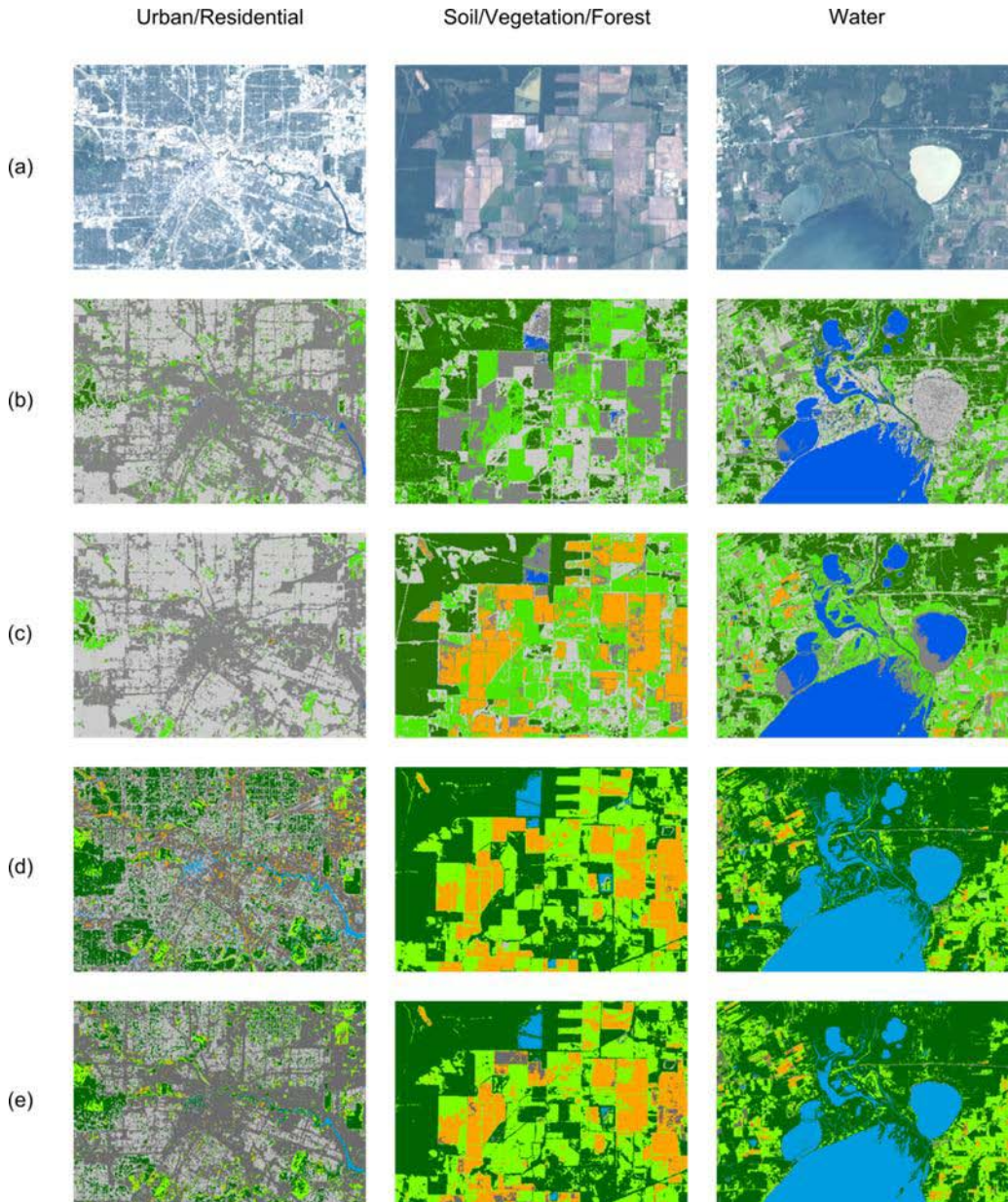


Figure 12. Side by side comparison of the classification results on three representative regions. (a) RGB band composite, (b) ArcGIS IsoCluster, (c) ArcGIS Maximum Likelihood, (d) ERDAS ISODATA, (e) ERDAS K-means

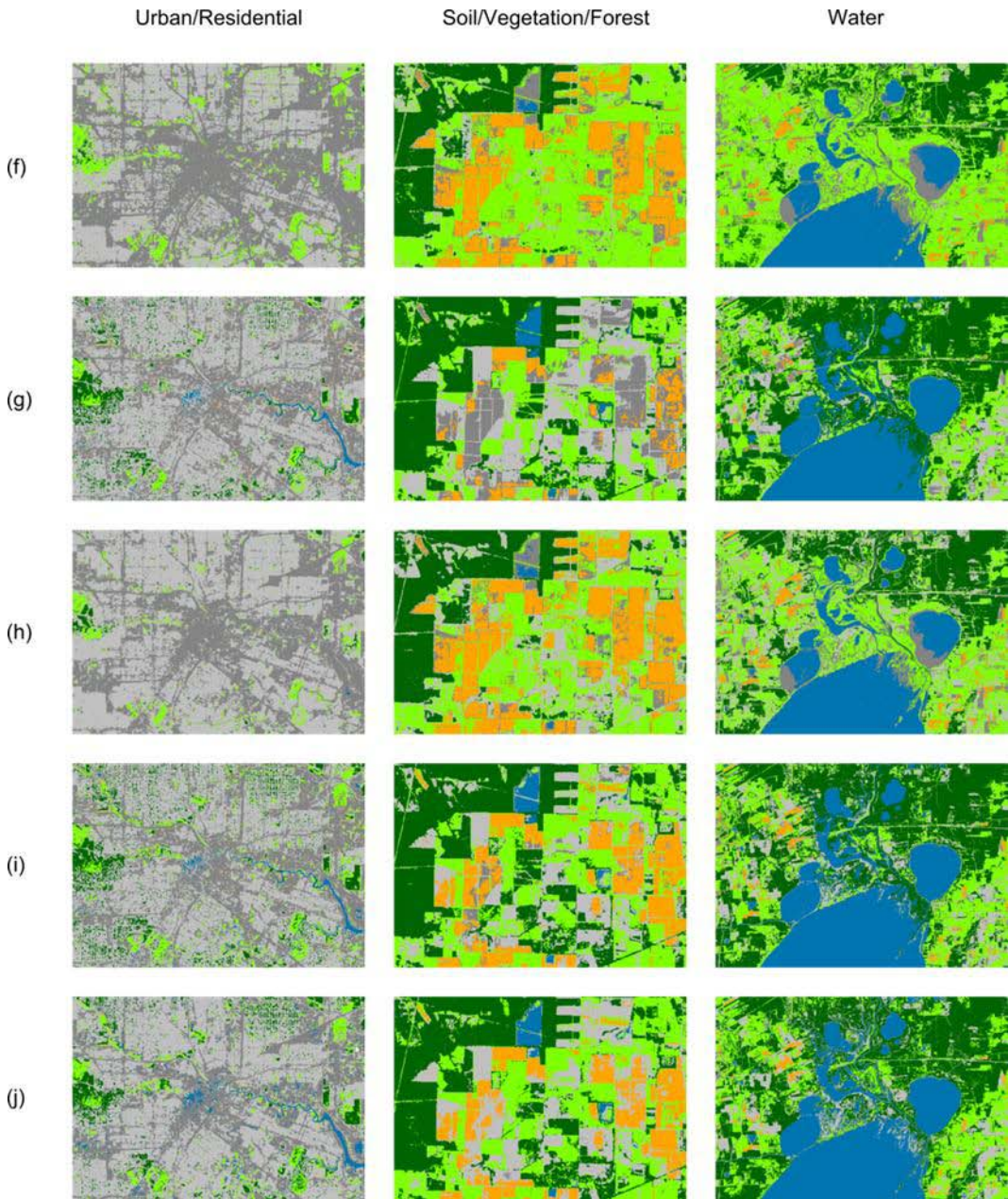


Figure 13. Side by side comparison of the classification results on three representative regions. (f) ERDAS Mahalanobis Distance, (g) ERDAS Minimum Distance, (h) ERDAS Maximum Likelihood, (i) ERDAS Spectral Angle Mapper, (j) ERDAS Spectral Correlation Mapper

Kappa coefficient agreement evaluation

Table 1 shows that all classification algorithms do not provide completely different results, with all kappa values being higher 0.6. All the kappa coefficients were statistically significant, with a p-value smaller than 0.05, but this was expected as the sample size was very large with n being the total number of pixels. However, there were differences in the distribution of the kappa

coefficients and patterns could be identified. The highest agreement, with a kappa value of 0.993, is between maximum likelihood algorithm for ArcGIS and ERDAS. This was expected, as both methods use the same process in assigning pixel to classes.

Two unsupervised algorithms, ERDAS K-means and ISODATA also have a high degree of similarity. This can be explained by the fact that both methods iteratively converge to solutions that minimize the total spectral distance between pixels and their cluster center. While K-means explicitly follow this objective by migrating the cluster centers to positions recalculated as centroids, ISODATA implicitly follows the same strategy with the merge/split operations. While, splitting a cluster will greatly reduce the total distance since it is performed on clusters that feature large variation, a merge operation will not significantly increase the total distance as it operates on clusters with small inter-centroid distance.

A high agreement can be observed among the triplet MD, SAM and SCM as the Euclidian distance to a training set centroid is correlated to the spectral angle. The correlation is heightened when the training sets are distributed with little variance around a certain spectral angle but span wide ranges of each band.

ERDAS Mahalanobis Distance shows more similarity with the maximum likelihood classifiers. This can be due to the fact that both methods assume a normal distribution of the pixels in the class.

The ArcGIS ISOCUSTER method has lower agreements with all the other methods including the expectedly similar ISODATA, mainly because it was not able to identify a distinct soil class.

Unexpectedly, the ERDAS Mahalanobis Distance has a kappa value of only 0.637 when compared with ERDAS Minimum Distance, showing that by choosing the simple Euclidean distance does not yield the same results as when more general distances are applied.

Table 3. Kappa statistic comparison

Method	IC	ML(A)	ID	KM	MhD	ML(E)	MD	SAM	SCM
IC	-	0.731	0.676	0.681	0.674	0.729	0.675	0.728	0.67
ML(A)	0.731	-	0.666	0.668	0.841	0.993	0.698	0.754	0.732
ID	0.676	0.666	-	0.907	0.639	0.667	0.741	0.778	0.73
KM	0.681	0.668	0.907	-	0.637	0.669	0.726	0.757	0.706
MhD	0.674	0.841	0.639	0.637	-	0.843	0.637	0.661	0.662
ML(E)	0.729	0.993	0.667	0.669	0.843	-	0.698	0.754	0.732
MD	0.675	0.698	0.741	0.726	0.637	0.698	-	0.861	0.819
SAM	0.728	0.754	0.778	0.757	0.661	0.754	0.861	-	0.876
SCM	0.67	0.732	0.73	0.706	0.662	0.732	0.819	0.876	-

CONCLUSION

We conclude the study with several remarks regarding the classification algorithms. The choice of classification algorithm affects has a strong effect on the results and one must make an informed decision when selecting the method. The most problematic situations have been identified as follows:

1. The Houston city downtown was often classified as water due to the shadowed areas.
2. Urban/residential/forest balance. Since residential areas consist of both buildings and trees it is challenging to separate the three classes.
3. Soil-urban confusion. Due to similar reflectance (in the majority of bands) of bare soil, asphalt and concrete, soil was often classified as urban or residential.
4. Soil-vegetation similarity. Soil is rarely completely vegetation free, therefore it will always be a challenge to decide whether a land parcel is cultivated or not.
5. Some algorithms did not differentiate forest from vegetation well enough. This was expected since they both have a similarly strong response on the green and NIR bands.

6. Shallow water, impure water, thin river lines and small lakes are sometimes hard to classify. The most frequent error classifies them as urban and/or residential.

None of the nine classification algorithms were able to avoid all of the above mentioned problems. Some algorithms were able to overcome a subset of these difficulties, others overcame a different subset and a few produced less errors overall. It is necessary to combine the solution of several algorithms in order to produce a good segmentation and one must understand how a particular classification method performs with respect to the desired goal. For this particular dataset, ERDAS ISODATA algorithm produced the most accurate classification. Not only it produces an overall good classification, but the few present errors may be easily rectified. These errors were located in the urban and residential areas. One error consisted in the downtown area being classified as water and another one consisted in the frequency of soil patches in the populated areas. This can be rectified by replacing the misclassified areas with the corresponding results produced by another algorithm. For this particular dataset, a good alternative for downtown Houston is the Mahalanobis distance classifier, and for the Soil, Maximum Likelihood.

The kappa coefficient assessment revealed relatively good agreement among all methods. Using kappa coefficients, we identified pairs and groups of methods with high agreements that in some instances could be explained by the logic of the underlying algorithms.

REFERENCES

- de Carvalho Jr. O. A., Meneses P. R., (2000), *Spectral Correlation Mapper (SCM): An Improvement on the Spectral Angle Mapper (SAM)*, AVIRIS Proceedings 2000.
- Cohen J. (1960), *A Coefficient of Agreement for Nominal Scales*, Educational and Psychological Measurement, volume 20, p. 37 - 46.
- Fu A., Sun G., Guo Z., Wang D. (2010), *Forest Cover Classification With MODIS Images in Northeastern Asia*, IEEE Journal of Selected Topics in Applied Earth Observations and Remote Sensing, volume 3, p. 178 – 189.
- Gamer M., Lemon J., Fellows I., Singh P. (2012), *Various Coefficients of Interrater Reliability and Agreement*, retrieved from <http://cran.r-project.org/package=irr>
- Goward S.N., Masek J. G., Williams D. L., Irons J. R., Thompson R. (2001), *The Landsat 7 mission: Terrestrial research and applications for the 21st century*, Remote Sensing of Environment, volume 78, p. 3 – 12.
- Lu D., Weng Q. (2006), *Use of impervious surface in urban land-use classification*, Remote Sensing of Environment, volume 102, p. 146 - 160.
- MacQueen J.B. (1967), *Some Methods for classification and Analysis of Multivariate Observations*, Proceedings of 5-th Berkeley Symposium on Mathematical Statistics and Probability, p. 281 - 297.
- Manandhar R., Odeh I.O.A., Ancev T. (2009), *Improving the Accuracy of Land Use and Land Cover Classification of Landsat Data Using Post-Classification Enhancement*, Remote Sensing, volume 1, p. 330 - 344.
- Pielke R A. (2005), *Land Use and Climate Change Science*, Science, volume 310, p. 1625 - 1626.
- de Pinho C. M. D., Fonseca L. M. G., Korting T. S., de Almeida C. M., Kux H. J. H. (2012), *Land-cover classification of an intra-urban environment using high-resolution images and object-based image analysis*, International Journal of Remote Sensing, volume 33, p. 5973 - 5995.
- R Core Team, (2013), *R: A Language and Environment for Statistical Computing*, Vienna, Austria: R Foundation for Statistical Computing, retrieved from <http://www.r-project.org>
- Stehman S. V. (1997), *Selecting and interpreting measures of thematic classification accuracy*, Remote Sensing of Environment, volume 62, p. 77-89.
- Hijmas R.J. (2014), raster: *Geographic data analysis and modeling*, retrieved from <http://CRAN.R-project.org/package=raster>
- Vannier C., Vasseur C., Hubert-Moy L., Baudry J. (2011), *Multiscale ecological assessment of remote sensing images*, Landscape Ecology, Springer Netherlands, volume 26, p. 1053 – 1069.
- Vibhute A., Bodhe S. K. (2012), *Applications of Image Processing in Agriculture: A Survey*, International Journal of Computer Applications, volume 52, p. 34 - 40.
- Viera A.J., Garrett J.M. (2005), *Understanding interobserver agreement: the kappa statistic*, Family Medicine, volume 37, p. 360-363.